Cochlear Mechanics

Academic and Research Staff
Professor Dennis M. Freeman, Professor Thomas F. Weiss, Dr. Alexander Aranyosi

Graduate Students
Chris Bergevin, Roozbeh Ghaffari, Kinuko Masaki, Scott Page

Mechanical Properties of the Cochlea

Sponsors
National Institutes of Health Grant R01 DC00238

Project Staff
Scott Page, Dr. Alexander Aranyosi, Professor Dennis M. Freeman, Professor Thomas F. Weiss

Introduction

The cochlea is responsible for transforming the mechanical vibrations of sound into neural signals that are sent to the brain. The physiological processes underlying this transformation are poorly understood. We have recently presented measurements showing that, in lower vertebrates, mechanical tuning of the sensory hair bundles of receptor cells plays a key role in determining how the cells respond to sound. However, the inner ears of mammals contain specialized structures, such as motile outer hair cells, that are not present in lower vertebrates but play a key role in cochlear function. To study such specializations we have adapted our measurement methods to investigate cochlear mechanics in mammals.

Sound-induced motions of cochlear structures

We have developed a preparation for studying the interaction of various cochlear structures *in situ* in response to vibration of the stapes, which is the input to the cochlea. Cochlear motions were measured in an isolated preparation of the temporal bone of a Mongolian gerbil (*Meriones unguiculatus*). Scala vestibuli was opened to allow optical access, but Reissner's membrane was left intact. The organ of Corti was illuminated from the scala tympani side using an optical fiber, and imaged with a high-power water-immersion objective. Images were collected using the computer microvision system we have developed (Aranyosi and Freeman, 2004) while the cochlea was driven by vibrating the stapes with a piezoelectrically-actuated probe. Using these images, we measured three-dimensional motions withnanometer-scale precision of numerous structures over a longitudinal segment of the cochlea. This preparation allowed us to measure displacements of the tectorial membrane (TM), hair bundles of outer and inner hair cells, the bodies of cells within the organ of Corti, Reissner's membrane, and fibers in the tunnel of Corti. Figure 1 shows images of various structures within the organ of Corti, including the TM and hair bundles of inner and outer hair cells. Because the measurement system is image-based, the motion of any structure that can be resolved in these images can be measured.

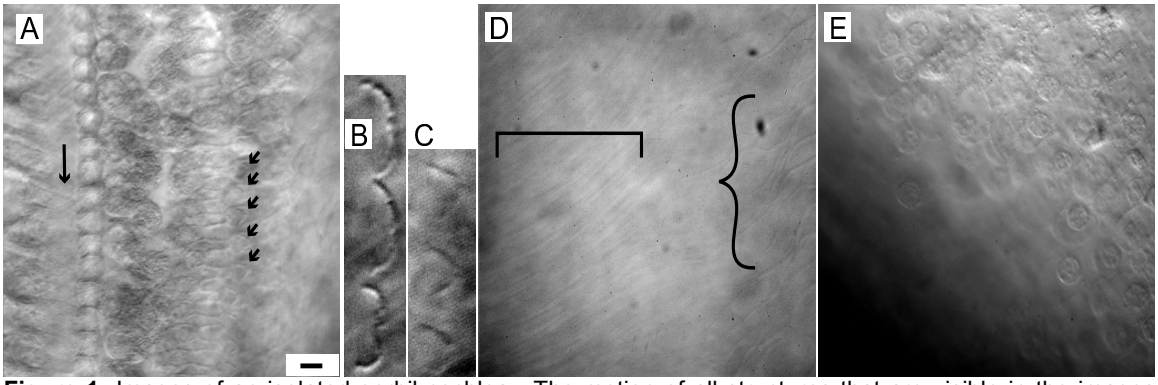

Figure 1: Images of an isolated gerbil cochlea. The motion of all structures that are visible in the images can be measured. **A**. A cross-sectional image through the organ of Corti. The long arrow points to a single efferent auditory nerve fiber crossing the tunnel of Corti. The short arrows point to the hair bundles of individual outer hair cells (OHCs). **B**. The hair bundles of three inner hair cells (IHCs). Individual stereocilia can be resolved within each bundle. **C**. The hair bundles of three OHCs. Although not resolved as well as IHC bundles, it is still possible to measure OHC bundle motion. **D**. Fibrillar structure of the TM. The straight bracket denotes the region where radial fibrils can be seen; the curly bracket denotes the region where the covering net is visible. **E**. Reissner's membrane. The cells and nuclei making up this membrane can be resolved.

Dynamic images reveal complex motions of the cochlea and its constituent structures. In five preparations we have seen a significant longitudinal component of motion of the organ of Corti in response to stapes motion (figure 2). Although this longitudinal motion may be affected by the presence of a hole in the cochlear apex, similar motions have been seen in response to electrical stimulation of an isolated apical turn of the cochlea (Karavitaki and Mountain, 2007), suggesting that this motion may be a natural vibrational mode of the organ. Moreover, the longitudinal motion of fibers in the tunnel of Corti in our preparation has a phase lead with respect to the motion of OHC bodies. One interpretation of this finding suggests that deformations basal to the measurement location induce fluid flow in the tunnel of Corti, and this fluid flow can rapidly propagate energy apically. Together, these results suggest that longitudinal motion may be a significant component of the cochlear response to sound, at least in the apex.

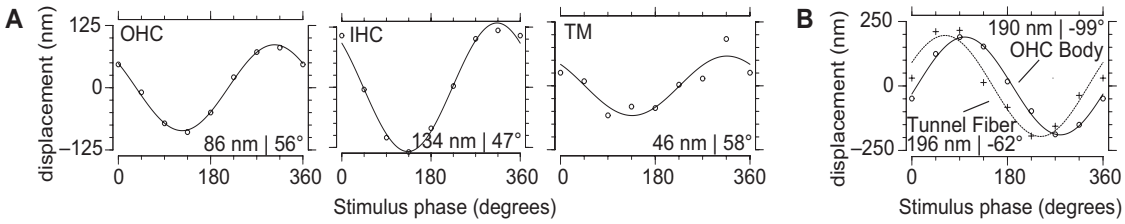

Figure 2: Longitudinal motion of the organ of Corti in response to a 400 Hz stimulus. A. Displacement of OHC bodies (left), IHC bundles (center), and TM marginal band (right). Longitudinal motion was largest at the IHCs, smallest at the TM, and nearly in phase at all locations. B. Displacement of an OHC body and an efferent fiber in the tunnel of Corti, from a different preparation. The efferent fiber had a phase lead with respect to the OHC body.

In addition to longitudinal motion, we have measured the relative motions of several structures in the radial direction (figure 3). The hair bundles of both inner and outer hair cells move relative to the bodies of outer hair cells, indicating that the acoustic stimulus is deflecting the hair bundles. Moreover, the TM moves radially out of phase with the bodies of OHCs. This counterphase motion is consistent with resonant-TM models of cochlear mechanics, and can serve to increase the shearing forces on hair bundles. However, in this preparation OHC bundle deflection and TM–RL shear displacement were not equivalent. This difference is similar to the difference

between RL displacement and IHC bundle deflection seen in a similar study (Fridberger et al, 2006), and indicates that the interaction between the TM and OHC bundles may be more complex than commonly believed.

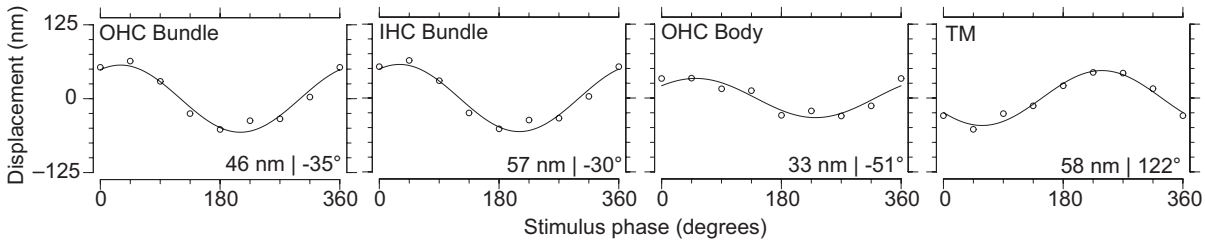

Figure 3: Radial motion of structures in an apical section of the organ of Corti in response to stapes vibration. The leftmost two plots show the displacement of hair bundles of outer and inner hair cells. Both displacements were nearly in phase, and the relative magnitude of displacement was somewhat larger for inner hair cell bundles. The center-right plot shows the displacement of OHC bodies. Compared to the displacement of bundles, OHC bodies moved less and lagged in phase. The rightmost plot shows the displacement of the marginal band of the TM. This portion of the TM moved nearly out of phase with the hair bundles and cell bodies. Stimulus was as described in figure 2.

The preparation has several aspects that make it valuable for studying cochlear micromechanics. First, stapes-driven motion simulates the *in vivo* drive to the cochlea. Second, the overall physical structure of the cochlea is kept intact to allow the propagation of traveling waves along the length of the cochlea. Third, endolymphatic space is not disrupted, so the organ of Corti is maintained in its normal fluid environment. These aspects ensure that the measured motions reflect the response of the cochlea to its natural stapes driven stimulus. The combination of stapes-driven motion with measurements of nanometer-scale three-dimensional motions of multiple structures over a longitudinal extent of the cochlea makes this preparation unique. This method will allow us to measure the interaction of the TM with hair bundles in three dimensions, and to look for evidence of a longitudinal TM traveling wave.

Improved Video Motion Measurement Techniques

Video methods of studying high-speed motion, as applied to cochlear mechanics and MEMS metrology, combine stroboscopic illumination and light microscopy to allow the simultaneous measurement of motion of multiple structures in multiple dimensions. These methods, pioneered by our group, have become widely adopted (Davis and Freeman, 1995; Karavitaki and Mountain, 2007; Hu et al, 1999; Hemmert et al, 2000; Cai et al, 2003; Fridberger and Boutet de Monvel, 2003). Although these methods have proved quite powerful, they have important limitations. Technical issues limit video methods to measuring motions driven by sinusoidal or near-sinusoidal signals. At the same time, since the methods depend on low-frequency image acquisition, the sensitivity of the measurements is limited by ambient low-frequency vibrations which are difficult to eliminate.

We have developed a new image-based technique that overcomes these limitations, allowing us to measure spontaneous motions and motion in response to complex stimuli, such as clicks or non-sinusoidal signals, with even greater sensitivity. The recent development of line scan cameras (introduced to popular culture by their use at the finish lines of Olympic racing events) is a windfall for cochlear micromechanics. The frame rates of commercially available line scan cameras approach 100 kHz, which should enable one-dimensional measurements of cochlear motion without requiring stroboscopic illumination (figure 4). Since the system does not alias motions down to low frequencies where table vibrations confound measurements, we can measure sub-nanometer motions — motions near the threshold of hearing.

Figure 4: Step response of a piezoelectric bimorph actuator imaged with 0.195 ms time resolution using a line scan camera. Each column of pixels in the image shows the edge of a bimorph viewed under a light microscope and recorded with a line scan camera. Adjacent columns of pixels indicate successive frames recorded at a frame rate of 5120 frames/s. The steady-state position change in response to a 5V step was 14 μm, but the bimorph oscillated at 430 Hz for more than 100 milliseconds with a peak-to-peak amplitude that initially exceeded 30 μm.

A Comparative Study of Otoacoustic Emissions

Project Staff

Chris Bergevin, Professor Dennis M. Freeman, Prof. Christopher Shera

Background

The ear not only detects ambient sounds, but actively emits sounds as well. These *otoacoustic emissions* (OAEs) reveal insight into the normal functioning of the auditory system, with applications in both research and clinical diagnosis. Although OAEs can be measured in the ears of most vertebrates, current models of OAE generation have focused primarily upon mammals, where unique features such as basilar membrane traveling waves and cell body somatic motility are believed to play a significant role. We have examined OAEs using identical methods in species that either have or lack these features to determine their contribution to OAE generation (figure 5).

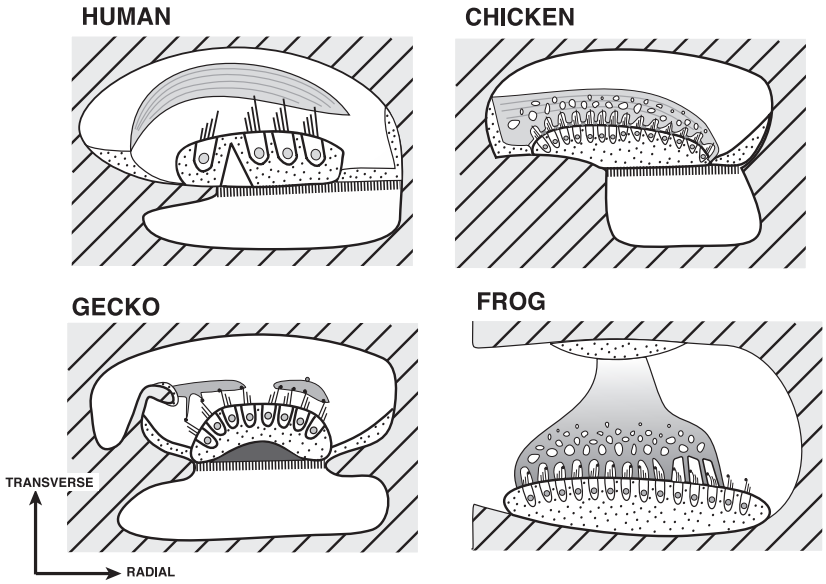

Figure 5: Simplified schematic of the inner ear anatomy of several species. Each image shows a cross-sectional view of the inner ear of one species. Notable features include bone (striped), fluid-filled spaces (white), hair cells containing hair bundles that project upward, and tectorial structures in close proximity to the bundles.

Evoked Otoacoustic Emissions

OAEs can either arise spontaneously or be evoked by an external acoustic stimulus. Evoked OAEs can be generated at the stimulus frequencies of single tones (SFOAEs) or by the intermodulation of two tones at distortion product frequencies (DPOAEs). Our results show that both DPOAEs and SFOAEs are largest below 2—3 kHz in species that lack traveling waves and somatic motility (figure 6).

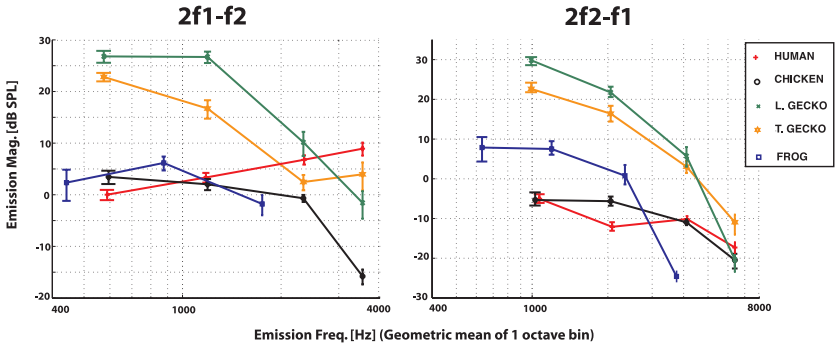

Figure 6: Comparison of DPOAE magnitudes across species. For all ears, two tones (f_1 and f_2) were presented to the ear at equal levels (65 dB SPL) and at a fixed frequency ratio (f_2/f_1=1.22). Each data point for a given species represents the magnitude averaged across individuals and frequency (in octave bins).

Mammalian OAEs have been proposed to arise from two fundamentally different mechanisms, one based upon linear reflection and the other on nonlinear distortion. Emission phase is used to distinguish between these two mechanisms. Our results (figure 7) indicate that the chicken ear behaves similarly to humans, suggestive of two mechanisms in the avian ear. However, emission mechanisms in the gecko and frog ears cannot be distinguished on the basis of phase. Consequently, it is not possible to determine for these species whether emissions result from two or only one mechanism.

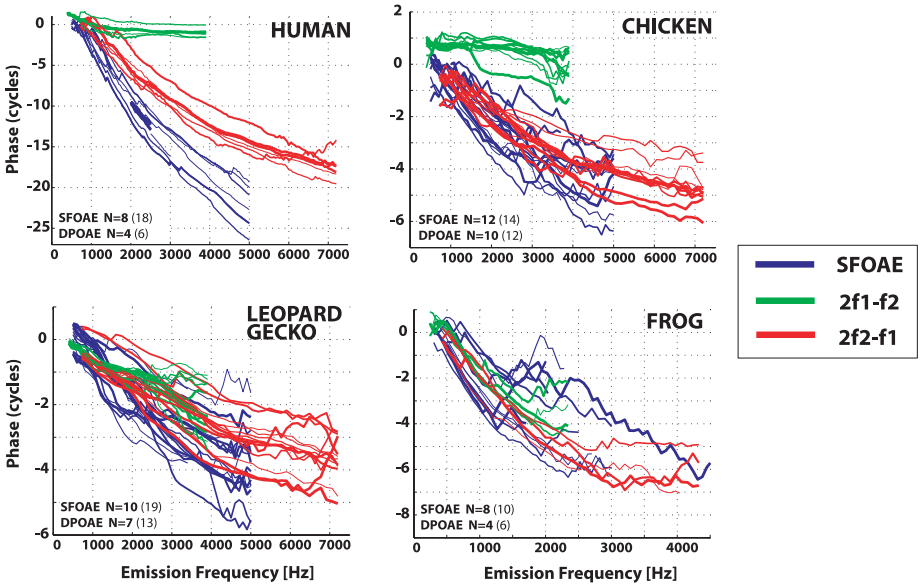

Figure 7: Comparison of SFOAE and DPOAE phase versus emission frequency. In all species, SFOAEs were evoked using a 40 dB SPL tone while DPOAEs were evoked using a pair of equal level tones at 65 dB SPL. In humans and chickens, the phase of 2f1-f2 emissions is relatively constant with frequency compared to the phase of 2f2-f1 and SFOAE emissions. In geckos and frogs, no such difference can be seen.

In all species, emissions exhibit significant delays, on the order of 1-10 ms or longer. These delays may arise from mechanical tuning properties of various inner ear structures, in addition to delays associated with the propagation of sound through the inner ear. Comparing SFOAE delays with measures of the sharpness of tuning derived from auditory nerve fibers shows that in all species except the frog, the frequency dependence of mechanical tuning correlates with the observed emission delays (figure 8).

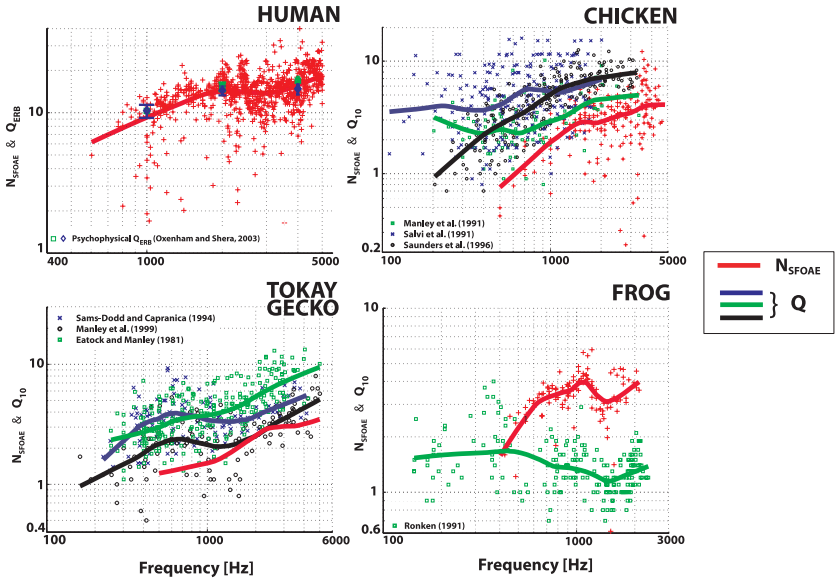

Figure 8: Comparison of SFOAE delays (expressed in dimensionless form as the number of stimulus cycles of delay) and auditory nerve fibers Q_{10dB} values. In all species except the frog, the two measurements exhibit a similar frequency dependence.

Evoked OAEs can grow non-monotonically with stimulus level. It has been proposed that an instantaneous nonlinear point source can account for this growth. By measuring an array of level-growth functions across species, our results indicate that numerous inconsistencies between OAEs and single-source model predictions (figure 9) argues in favor of the multiple-source theory.

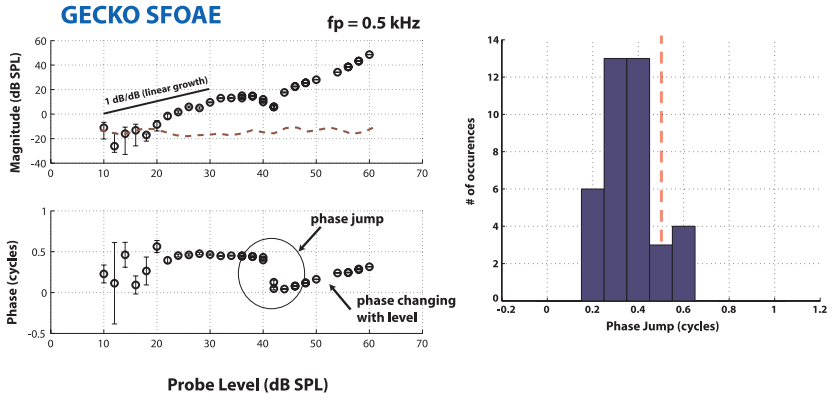

Figure 9: Non-monotonic SFOAE growth in an individual gecko ear. Histogram shows the distribution of phase jumps across a notch in all species. One of the single-source model predictions is that the phase jump across a notch is strictly 1/2 cycle, in clear contrast to the data.

Summary

Our measurements reveal that the processes by which OAEs are generated depend on the underlying anatomy in a complex manner. These results show that properties of OAEs that had previously been attributed to mammalian-specific auditory features exist in a variety of vertebrates which lack those features. Consequently the contribution of properties such as outer hair cell motility and cochlear traveling waves to OAE generation is not as direct as previously believed.

Publication

Journal Articles, Published

Masaki, K., T. F. Weiss, and D. M. Freeman, "Poroelastic bulk properties of the tectorial membrane measured with osmotic stress," *Biophys J* **91**:2356-70, 2006.

Hong, S. S. and D. M. Freeman, "Doppler optical coherence microscopy for studies of cochlear mechanics," *J Biomed Opt* **11**:045014, 2006.

Anvari, B., W. E. Brownell, D. M. Freeman, and M. Ulfendahl, "Photonics in the auditory system," *J Biomed Opt* **12**:021001, 2007.

Meeting Papers, Published

Bergevin, C., D. M. Freeman, and C. A. Shera, "Otoacoustic emissions in humans, birds, lizards, and amphibians: a comparative study reveals differences in emission generation mechanisms," presented at the *Thirtieth Annual Midwinter Meeting of the Association for Research in Otolaryngology*, Denver, CO, 2007.

Bergevin, C., "Are basilar membrane traveling wave delays necessary for long OAE delays?," presented at *Workshop 8: The Auditory System*, Mathematical Biosciences Institute, Columbus OH, 2007.

Theses

Masaki, Kinuko, *Measuring material properties of tectorial membranes from normal and genetically modified mice*, Ph.D. Thesis, Harvard-MIT Division of Health Sciences and Technology: MIT, 2006.

Bergevin, Christopher, *Comparative approaches to otoacoustic emissions: Towards an understanding of why the ear emits sound*, Ph.D. Thesis, Harvard-MIT Division of Health Sciences and Technology, MIT 2007.